

RESEARCH

Open Access



Biomechanical comparison of three tibial tunnel positions for PCL reconstruction: a 3D finite element analysis

Siman Tian¹, Yi Zheng¹, Yubin Long², Yingzhen Niu¹, Zhikuan Li¹ and Jiangtao Dong^{1*}

Abstract

Purpose To compare the biomechanical properties of the graft during PCL reconstruction by three-dimensional finite element analysis of the PCL trans-tibial reconstruction technique with three different tibial bony channel exit positioning points, to determine which method of positioning is better able to avoid wear and tear between the graft and bony channel, and to reduce the failure rate of the PCL reconstruction.

Methods This is a study limited to computational simulation and based on data from a single anatomical model. Thirty-year-old male volunteers were selected. A three-dimensional knee joint model consisting of the distal femur, the proximal tibiofibula and the posterior cruciate ligament was established based on CT scanning and three-dimensional reconstruction of the left knee joint. According to the different positioning points of the tibial tunnel exit, the PCL model of tibial side PCL anatomical region center point reconstruction, the PCL model of Fanelli suggested point (i.e., 10 mm below and 5 mm lateral to the PCL anatomical point) reconstruction, and the PCL model of tibial side posterior posterior joint capsule distal anticompromise and posterior mediastinum reference positioning point (i.e., 5 mm above the posterior capsule distal retropubic, 5 mm medial to the posterior mediastinum) reconstruction were established (respectively designated as Model 1, Model 2, and Model 3). The diameter of the entire graft was set uniformly at 7 mm. With the knee flexed at 90° and the midpoint of the line connecting the medial and lateral apices of the tibial intercondylar ridge as the reference point, a standardized backward thrust displacement of 5 mm was applied to simulate a posterior knee drawer test with all proximal femoral degrees of freedom constrained. The model overall Mises stress, tibial plateau Mises stress, PCL Mises stress, PCL contact Cpress stress, PCL contact stress and PCL contact effective area were measured.

Results Simulated posterior drawer tests demonstrated that Model 3 exhibited a substantial reduction in PCL contact Cpress stress (22.57 MPa) compared to Model 1 (32.93 MPa) and Model 2 (29.86 MPa). Additionally, the ratio of contact force (277.48 N) to effective graft-tibial contact area (50.19 mm²), representing the contact force per unit area, was also the lowest in Model 3 compared to Model 1 (213.88 N/17.65 mm²) and Model 2 (470.77 N/63.75 mm²). These findings indicate that Model 3 significantly reduced frictional loads between the graft and tibia, highlighting its biomechanical optimization potential. Further analysis revealed that Model 3 also displayed the lowest tibial plateau Mises stress (48.80 MPa). However, its PCL tensile stress (69.71 MPa) was significantly higher than that of Model 1

*Correspondence:
Jiangtao Dong
djt@hebmu.edu.cn

Full list of author information is available at the end of the article



© The Author(s) 2025. **Open Access** This article is licensed under a Creative Commons Attribution-NonCommercial-NoDerivatives 4.0 International License, which permits any non-commercial use, sharing, distribution and reproduction in any medium or format, as long as you give appropriate credit to the original author(s) and the source, provide a link to the Creative Commons licence, and indicate if you modified the licensed material. You do not have permission under this licence to share adapted material derived from this article or parts of it. The images or other third party material in this article are included in the article's Creative Commons licence, unless indicated otherwise in a credit line to the material. If material is not included in the article's Creative Commons licence and your intended use is not permitted by statutory regulation or exceeds the permitted use, you will need to obtain permission directly from the copyright holder. To view a copy of this licence, visit <http://creativecommons.org/licenses/by-nc-nd/4.0/>.

(41.03 MPa) and Model 2 (40.90 MPa), suggesting that while Model 3 minimizes friction dependency, it primarily transfers loads through graft tension.

Conclusion Compared with the anatomic regional center point and Fanelli point reconstruction PCL, the grafts of the soft tissue reference tibial localization reconstruction PCL method were subjected to greater tensile forces, but they had significantly lower friction with the tibia and were able to reduce contact wear with the tibia. This can enhance long-term patient outcomes. Our study offers crucial biomechanical evidence for optimizing tunnel positioning in PCL reconstruction, propelling the advancement of surgical techniques.

Keywords Posterior cruciate ligament reconstruction, Three-dimensional finite element (FEM), Tibial tunnel, Posterior joint capsule, Posterior septum

Introduction

The posterior cruciate ligament (PCL) injury is a common knee ligament injury, typically caused by high-energy trauma or sports-related activities. The incidence is 0.65–3% in the athletic population and 1.8/100,000 in the general population [1]. In recent years, studies utilizing musculoskeletal modeling have revealed the biomechanical effects of PCL injuries on the knee joint [2, 3]. These studies demonstrate that PCL deficiency leads to increased posterior tibial displacement, redistribution of internal knee loads, elevated forces on posterolateral corner structures, and heightened tibiofemoral and patellofemoral contact forces. Such biomechanical alterations may elevate the risk of osteoarthritis. Therefore, we assert that arthroscopic posterior cruciate ligament reconstruction (PCLR), aimed at restoring knee joint stability, is an effective treatment for both acute and chronic PCL injuries. However, studies have reported a 53% complication rate after PCL reconstruction [4], including joint stiffness or limited mobility, neurologic or vascular injury, and graft failure. According to the study, the graft failure rate was as high as 46.7% [5]. Currently, the causes of PCLR failure are varied, and the positioning of the tibial tunnel is considered a critical factor, but scholars are still controversial about the optimal location of the osteopathic tract [6, 7].

In practical surgery, correctly choosing the tibial tunnel outlet remains a challenging issue. Anatomical-based PCLR is the most commonly used method, which involves positioning the tibial tunnel outlet at the center of the PCL anatomical region [8, 9]. The advantage of this method is that it aims to mimic the natural anatomical structure of the PCL as closely as possible, restoring the biomechanics of the knee joint. However, this technique also has some drawbacks. First, when the PCL is reconstructed via the tibia, the graft folds back through the tibial bone tunnel to the medial femoral condyle to form an acute pinch angle at the proximal tibia, and the researchers believe that the graft will rub against the tibial bone tunnel postoperatively, leading to graft abrasion, or the “killer turn” effect [10]. Positioning at the anatomical center point does not better minimize this effect. Second,

compared with the complete tibial side anatomical footprint of the PCL [11], the reconstructed graft cannot fully cover the entire footprint area. Additionally, the PCL's anatomical characteristics are complex, and it is difficult to locate the true anatomical center on the coronal and sagittal planes when preserving the ligament's remnant [9]. Some surgeons opt to remove the remnant to obtain the center of the footprint area. However, studies suggest that preserving the ligament remnants and adjacent soft tissue during PCLR may be more beneficial for graft survival and the recovery of ligament function because the preservation of its internal neurovascular structures and proprioceptive vesicles promotes graft healing and revascularization [12, 13].

Based on this, some scholars have proposed establishing a low-positioned tibial tunnel [14–16]. Fanelli [17] suggested positioning the tibial tunnel in the distal and lateral regions of the PCL tibial footprint to create a low-position tibial tunnel, increasing the sharp angle formed between the graft and the tibial plateau, thereby reducing the “killer turn” effect. Wang [18] and others have demonstrated through three-dimensional finite element analysis that reconstructing the PCL in the Fanelli region, particularly 10 mm below the PCL anatomical point and 5 mm laterally, results in the lowest peak stress on the graft. However, despite the mechanical and finite element analysis showing that the Fanelli point can effectively reduce the “killer turn” effect, this approach deviates from the traditional anatomical footprint, and the tibial tunnel outlet is positioned closer to neurovascular structures, thus increasing the risk of damage. Moreover, Wang [18] and others confirmed that although this positioning effectively addresses the “killer turn” issue, it results in a greater posterior translation of the tibia.

To address these issues, our research team has proposed a new tibial tunnel positioning method, which utilizes the distal fold of the posterior joint capsule and the posterior septum as reference landmarks to establish the tibial tunnel's soft reference positioning technique. Previously, the establishment of the bone channel was mainly based on bony structures such as the tibial plateau as a reference mark, but there are large differences in bony

structures between patients, resulting in a high variability in the position of the bone channel established by using the digital distance of the bony structures as a reference, which is not conducive to the standardization of the clinical technique. By utilizing the anatomical features of the distal fold of the posterior joint capsule and the posterior septum, we can accurately position the tibial tunnel outlet. We position the tibial tunnel 5 mm above the distal fold of the posterior joint capsule and 5 mm medially from the posterior septum, placing the tibial tunnel outlet within the PCL anatomical region and lower than the traditional anatomical center. We believe that this position can not only reduce the “killer turn” effect, avoids graft wear, and increases graft longevity; it also places the tibial tunnel within the preserved PCL anatomical footprint area, better preserving the PCL remnants and adjacent soft tissues such as the posterior septum, with high clinical reproducibility [19, 20].

We have confirmed the advantages of soft tissue reference positioning method through anatomical and clinical studies, but mechanical experiments have not yet been conducted for verification. Three-dimensional finite element analysis (FEA) enables precise comparison of micromechanical differences and quantification of biomechanical parameters that are difficult to obtain from traditional experiments through a controlled mechanical environment that is non-invasive, reproducible and controllable. Therefore, this study aims to construct knee joint models based on three different tibial tunnel positioning methods using FEA. These models include: the tibial side PCL anatomical region center point reconstruction model, the Fanelli point reconstruction model, and the tibial side soft tissue reference positioning point reconstruction model. By simulating the posterior drawer test, we will compare the mechanical characteristics of these three models. We hypothesized that the soft-tissue tibial tunnel positioning method is superior to the other two positioning methods in terms of optimizing mechanical properties and reducing adverse effects. We expect this mechanical analysis to provide more scientific surgical guidance for anatomic reconstruction of the PCL.

Materials and methods

Experimental subjects

Given the high incidence of PCL injuries in young males, this study recruited a 30-year-old healthy male volunteer (height 175 cm, weight 70 kg, BMI 22.9 kg/m²). All images and data were obtained with his consent. Inclusion criteria were: no history of knee trauma or surgery (confirmed clinically and by imaging), and no congenital deformities. The volunteer lay supine with knees extended. CT scans of the left knee were taken using a Siemens Somatom Definition AS 128 CT scanner (slice thickness 0.6 mm, tube voltage 120 kV), and MRI scans

using a 3T Magnetom Skyra system (T1/T2 sequence slice thickness 1.0/3.0 mm). Two radiologists confirmed all images matched classic anatomical features.

Construction of the knee joint 3D finite element model

CT images were used for the 3D reconstruction of the bone structures (tibia, fibula, femur, and patella). MRI images were used for the 3D reconstruction of the soft tissues (ligaments, menisci, and cartilage). CT and MRI scan data were imported into MIMICS (Materialise, Ver. 21.0) modeling software to automatically generate the original 3D knee joint model and two orthopaedic surgeons manually segmented the soft tissues to ensure anatomical accuracy, and the data were saved in STL format. The STL file was then imported into Geomagic Wrap (Geomagic Inc., USA, Ver. 2021) for editing to smooth the surface of the model. The processed model was exported as an STL file and further imported into SolidWorks software (Dassault Systemes Inc., France, Ver. 2021) for assembly and structural optimization. The model was meshed using ANSA software (Ver. 2021), with tetrahedral elements and shell elements. Mesh mass aspect ratios were within 5, minimum height 0.2, cell lengths between 0.2 and 2, quadrilateral cell angles 30–150, and triangular cell angles 20–140. The results were stabilized by grid sensitivity analysis when the average cell size was refined to 1 mm (0.2–2 mm). The tetrahedral elements used were C3D4, and the shell elements were S3. The entire model consisted of 2,561,351 solid elements. Set the coefficient of sliding friction for graft-bone channel interface contact 0.05. The femoral and tibial ends were separately fixed by binding constraints simulating interface screw fixation.

The PCL was removed from the model to simulate a knee joint with a ruptured PCL. On the knee joint model without a PCL, three different PCL reconstruction models were constructed based on different tibial tunnel outlet positions (Positioning of localization points to be determined by two specialized orthopaedic surgeons). Model 1 was created by positioning the tibial tunnel outlet at the center of the PCL anatomical footprint. Model 2 was created by positioning the tibial tunnel outlet at the Fanelli point, 10 mm below the PCL anatomical point and 5 mm laterally. Model 3 was created by positioning the tibial tunnel outlet at the soft tissue reference point, 5 mm above the distal fold of the posterior joint capsule and 5 mm medially from the posterior septum (Figure 1). Tibial tuberosity channel angle of 45°. All three models were positioned to establish the femoral osseous channel by the clock-disc method. The internal opening of the channel was located at 10 o'clock (left knee) in the intercondylar recess. The reconstructed grafts in all models were round and 7 mm in diameter.

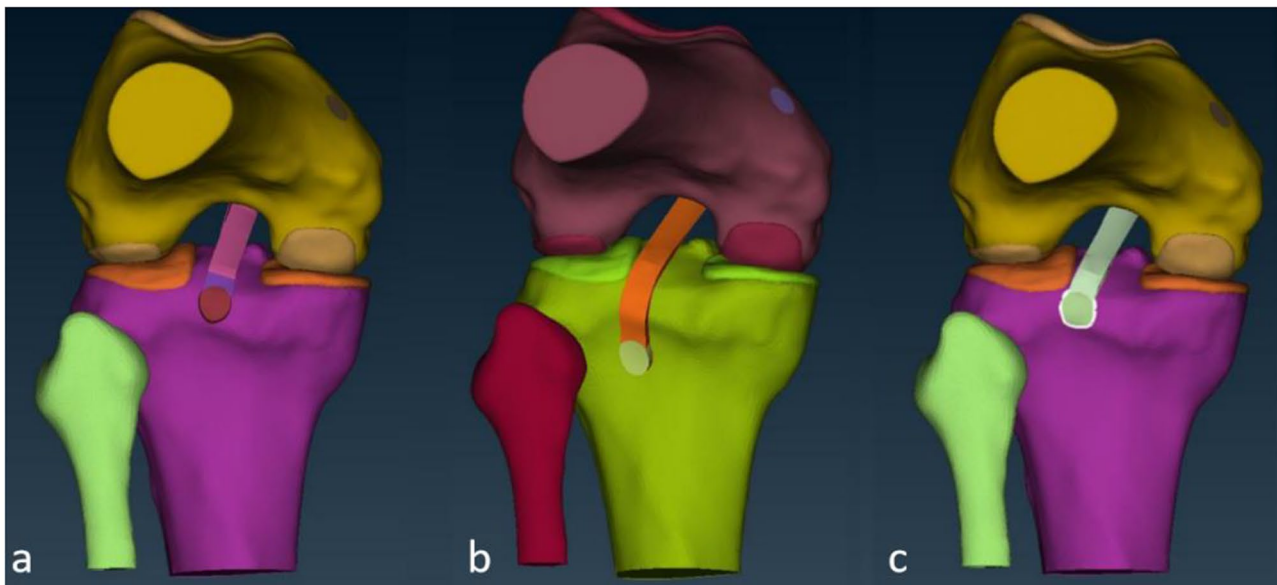


Fig. 1 Posterior view of the 3D model of the knee joint. **a.** Model 1 / Anatomical Region Center Point-based PCLR Model; **b.** Model 2 / Fanelli Point-based PCLR Model; **c.** Model 3 / Soft Tissue Reference Point-based PCLR Model

Material properties

The material properties for each part of the model were determined based on previously published literature [18, 21, 22]: the elastic modulus of cortical bone was 17,000 MPa with a Poisson's ratio of 0.36; the elastic modulus of cancellous bone was 350 MPa with a Poisson's ratio of 0.25; the elastic modulus of articular cartilage was 5 MPa with a Poisson's ratio of 0.46; the elastic modulus of the meniscus was 59 MPa with a Poisson's ratio of 0.49; the elastic modulus of ligaments was 390 MPa with a Poisson's ratio of 0.40; and the elastic modulus of grafts was 260 MPa with a Poisson's ratio of 0.30.

Measurement methods

The PCL reconstruction model was simulated with a posterior drawer test at 90° knee flexion angle. Using the midpoint of the line connecting the medial and lateral apex of the tibial intercondylar ridge as a reference point, a certain force was applied to the tibia until a standard posterior thrust displacement of 5 mm was achieved (The magnitude of the displacement obtained when the rear drawer experiment was carried out by imaging measurements), with all proximal femoral degrees of freedom constrained. Measure the overall von Mises stress, tibial plateau von Mises stress, PCL von Mises stress, PCL contact Cpress stress, contact resultant force, and contact effective area for all three models. Record the maximum values and compare them to evaluate the graft's loading conditions. Stress calculations were done through the implicit analysis Standard module of the Abaqus software (Ver. 6.13). Tibial plateau Mises stress is the stress generated on the tibial plateau by the interaction force

Table 1 Data table for simulation analysis of three models

	Model 1	Model 2	Model 3
Model overall Mises stress (Mpa)	55.83	53.08	69.71
Tibial plateau Mises stress (Mpa)	55.83	53.08	48.80
PCL Mises stress (Mpa)	41.03	40.90	69.71
PCL contact Cpress stress (Mpa)	32.93	29.86	22.57
PCL contact force (N)	213.88	470.77	277.48
PCL contact effective area (mm ²)	17.65	63.75	50.19

between the graft and the tibia during the simulated posterior drawer experiments. PCL Mises stress refers to the overall stresses on the graft, including the tensile force exerted on the graft itself as well as the friction force generated with the tibia during the displacement process. Where the friction generated between the graft and the tibia produces a stress on the graft that is the PCL Contact Cpress stress. The ratio of the PCL contact Cpress to the effective area of PCL contact was used to evaluate the contact friction generated between the graft and the tibia per effective area.

Results

The results of the force measurement for each model, based on the simulation of the posterior drawer test, are shown in Table 1. For the overall Mises stress of the models (Fig. 2), Model 3 experienced the highest force, at 69.71 MPa, followed by Model 1 with a force of 55.83 MPa, and Model 2 with the lowest force of 53.08 MPa.

For the Mises stress on the tibial plateau (Fig. 3), which is due to the interaction between the PCL and the tibia, Model 3 experienced the lowest force, at 48.80 MPa.

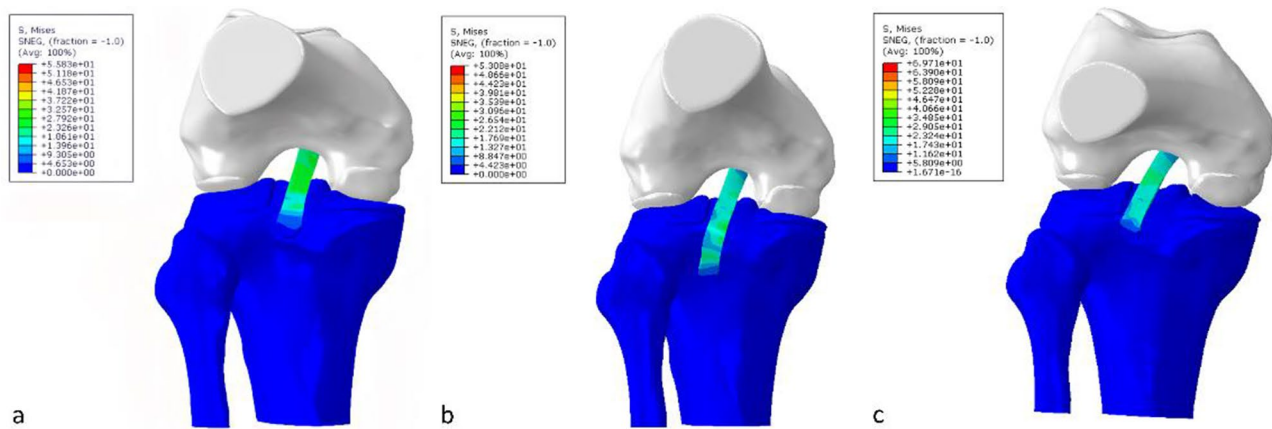


Fig. 2 Model overall Mises stress distribution. **a.** Model 1 overall Mises stress distribution; **b.** Model 2 overall Mises stress distribution; **c.** Model 3 overall Mises stress distribution

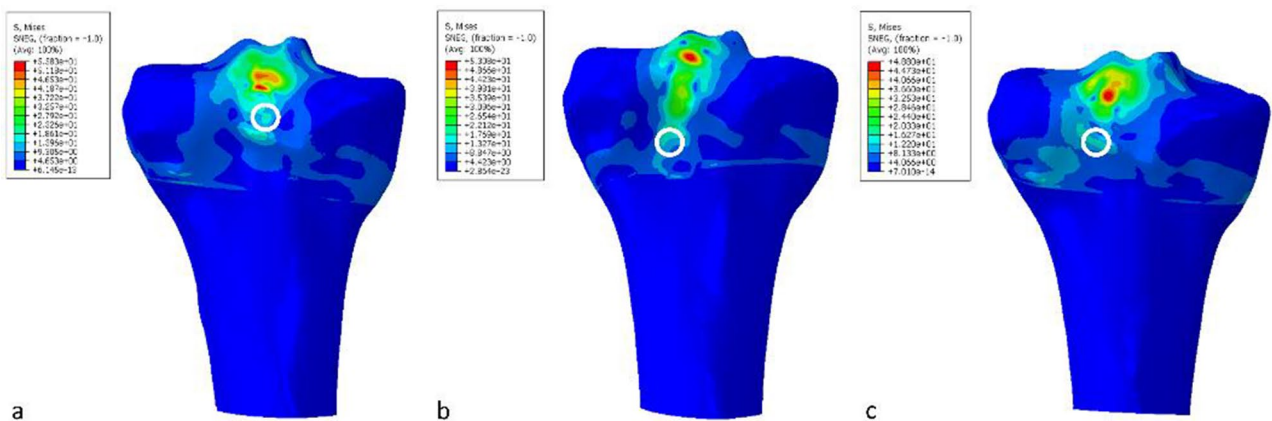


Fig. 3 Mises stress distribution of the tibial plateau. **a.** Mises stress distribution of the tibial plateau of model 1; **b.** Mises stress distribution of the tibial plateau of model 2; and **c.** Mises stress distribution of the tibial plateau of model 3. The white circle is the location of the tibial tuberosity tract exit

Model 1 and Model 2 had forces of 55.83 MPa and 53.08 MPa, respectively, which correspond to their overall Mises stress values. This indicates that the primary force on the tibial plateau in models 1 and 2 comes from the interaction between the PCL and the tibia, i.e., contact friction force, while the tibial plateau of model 3 was subjected to the least contact friction force.

For the Mises stress on the PCL (Fig. 4), Model 2 had the smallest value, at 40.90 MPa; Model 1 had a mid-range value of 41.03 MPa; and Model 3 had the highest value, at 69.71 MPa, which corresponds to the overall Mises stress of this model. This shows that the maximum force in Model 3 originates from the stresses applied to the grafts. The Mises stress on the PCL is mainly divided into tensile force and pressure friction force, with the pressure friction force represented by the PCL contact Cpress stress. The PCL contact Cpress stress is smallest in Model 3, at 22.57 MPa, while in Model 1 and Model 2, it is 32.93 MPa and 29.86 MPa, respectively (Fig. 5). This indicates that although the grafts in Model 3 were

subjected to greater overall stresses than those in Models 1 and 2, the pressure-friction forces were less than those in the remaining two models, so the grafts in Model 3 were mainly subjected to the tensile forces on the ligaments. The grafts in models 1 and 2 were subjected to greater frictional forces compared to model 3.

Additionally, considering the data for the PCL contact force and effective contact area (Fig. 6, 7), Model 3 has lower contact force (277.48/50.19) compared to Model 1 (213.88/17.65) and Model 2 (470.77/63.75). This is consistent with the PCL contact Cpress stress data.

Discussion

This study compared the biomechanical characteristics of grafts in three different tibial tunnel outlet positioning methods for PCL reconstruction using 3D finite element analysis. The results revealed that, compared to the anatomical center point and Fanelli point tibial positioning methods, the soft tissue reference tibial positioning method, which uses the distal fold of the posterior joint

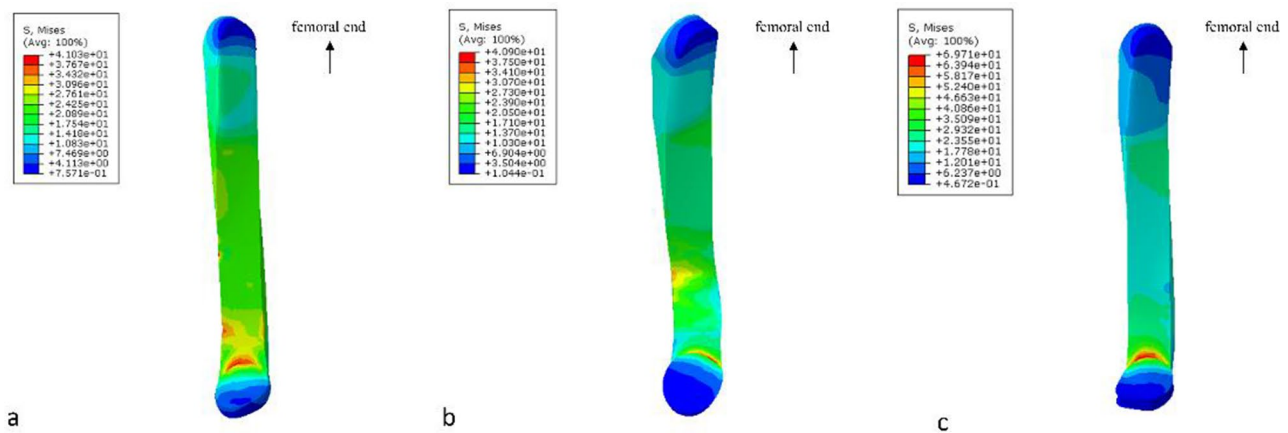


Fig. 4 PCL Mises stress distribution plots. **a.** Model 1 PCL Mises stress distribution plots; **b.** Model 2 PCL Mises stress distribution plots; **c.** Model 3 PCL Mises stress distribution plots

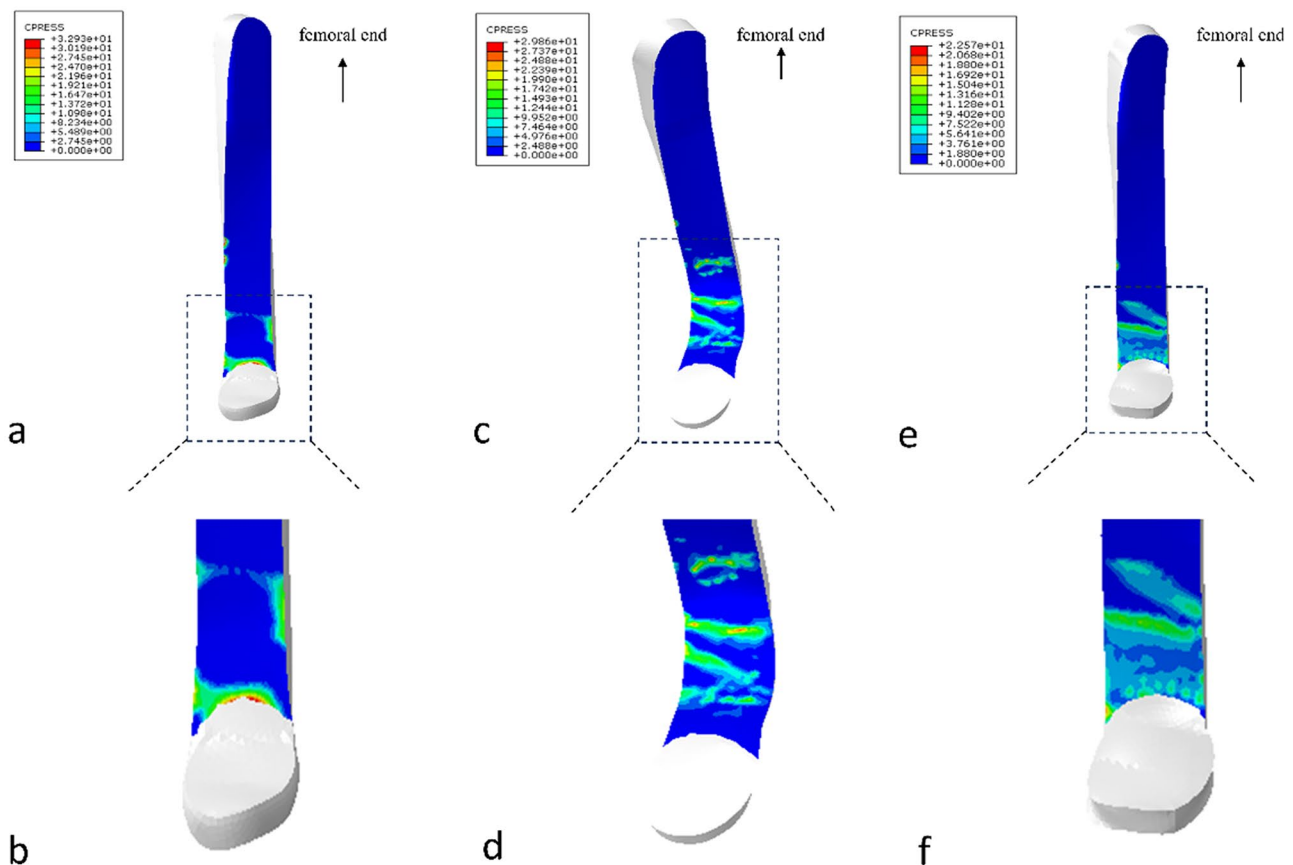


Fig. 5 PCL contact Cpress stress distribution plots. **a.** Model 1 PCL contact Cpress stress distribution plots; **b.** Model 1 Enlarged view of critical areas of PCL contact Cpress stress distribution plots; **c.** Model 2 PCL contact Cpress stress distribution plots; **d.** Model 2 Enlarged view of critical areas of PCL contact Cpress stress distribution plots; **e.** Model 3 PCL contact Cpress stress distribution plots; **f.** Model 3 Enlarged view of critical areas of PCL contact Cpress stress distribution plots

capsule and the posterior septum, creates minimal friction between the graft and the tibia, which reduces the risk of wear and tear of the graft and thus improves the graft survival rate. This finding theoretically suggests that the soft-tissue-referenced tibial osteopathic tract

localization method we advocate for PCL reconstruction may improve the surgical success rate, improve patient prognosis, and provide a new option for surgical approaches to PCLR.

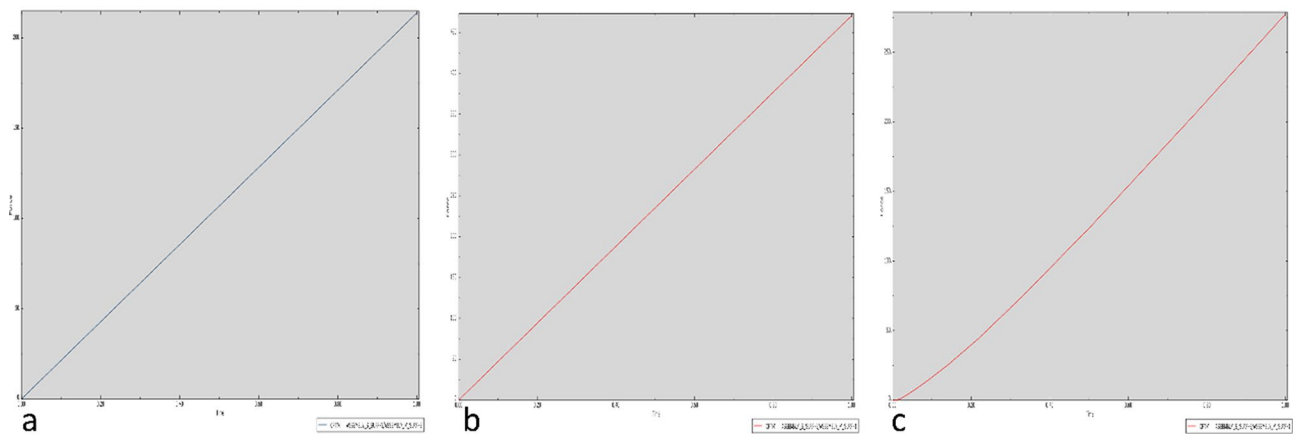


Fig. 6 PCL contact cohesion diagram. **a.** Model 1 PCL contact cohesion diagram; **b.** Model 2 PCL contact cohesion diagram; **c.** Model 3 PCL contact cohesion diagram

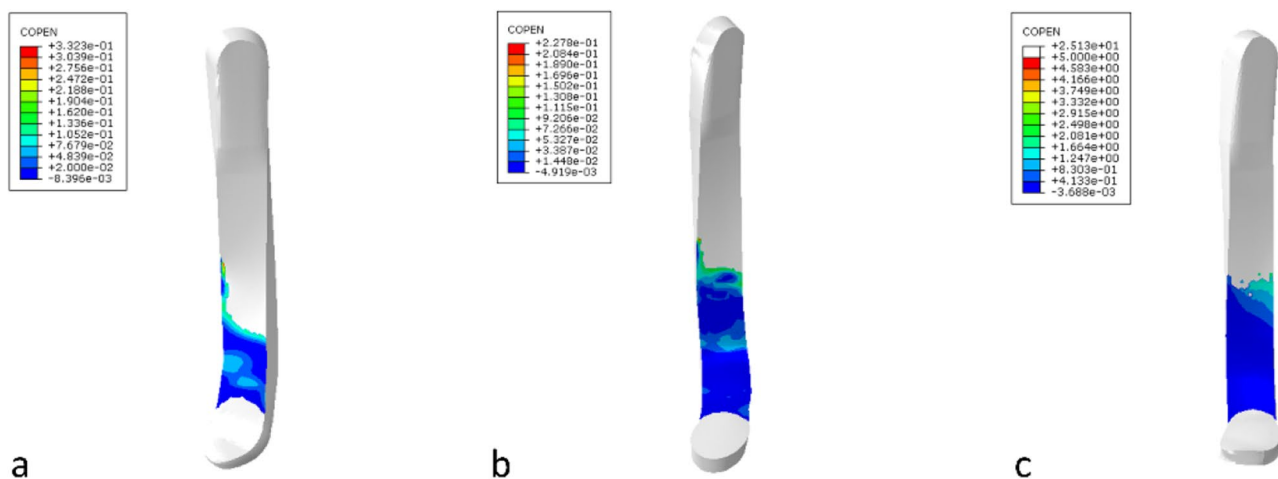


Fig. 7 Schematic of PCL contact effective area. **a.** Schematic of Model 1 PCL contact effective area; **b.** Schematic of Model 2 PCL contact effective area; **c.** Schematic of Model 3 PCL contact effective area

In recent years, with the rapid development of computer technology, three-dimensional finite element analysis has been widely used in the field of biomedical engineering. Through 3D finite element modeling, researchers have been able to systematically evaluate the effects of different surgical techniques, graft materials, and bone channel locations on the biomechanical properties of the knee joint. Most of the literature on assessing the “killer turn” effect in PCL reconstruction by 3D finite element analysis has focused on reducing this effect by changing the orientation and angle of the tibial tunnel [22–24].

The overall Mises stress of the models represents the maximum stress experienced by the entire model. The results showed that Model 3 (soft tissue reference tibial positioning) had the highest stress, followed by Model 1 (anatomical region center point) and Model 2 (Fanelli point). The maximum stress in Model 3 was the PCL Mises stress, while the maximum stress in Models 1

and 2 was the tibial plateau Mises stress. The tibial plateau Mises stress represents the maximum force on the tibial plateau, which, in the 3D model during the posterior drawer simulation, is primarily due to the interaction force between the graft and the tibia, i.e., the frictional force between them. Many studies have shown that this tibial-based PCL reconstruction technique inevitably leads to the “killer turn” effect [21, 22, 25, 26], which refers to the sharp angle formed at the proximal tibia when the graft passes through the tibial tunnel and turns back to the femoral medial condyle. The “killer turn” can cause friction between the graft and the bony structure at the proximal outlet of the tibial tunnel, leading to graft wear and thinning [22, 23, 25, 27]. Our results show that the tibial plateau Mises stress was smallest in Model 3, intermediate in Model 2, and largest in Model 1. This indicates that the soft tissue reference positioning method optimizes the contact between the PCL and tibia, significantly reducing the contact friction force

between the graft and tibial plateau, and more effectively minimizing the “killer turn” effect, thereby lowering the risk of graft wear. Moreover, the tibial tunnel outlet positioned at the Fanelli point experiences less friction than the anatomical region center point positioning, suggesting that establishing a lower tibial tunnel can effectively reduce the “killer turn” effect, consistent with previous studies [14, 18, 28].

For the PCL Mises stress, which represents the maximum stress experienced by the PCL as a whole, Model 3 had the highest stress, Model 1 had intermediate stress, and Model 2 had the lowest stress. It is also noteworthy that the PCL contact Cpress stress (contact friction force) in Model 3 was significantly smaller than in Models 1 and 2. Combining these results with the overall Mises stress and tibial plateau Mises stress, we find that the graft in the soft tissue reference positioning method (Model 3) is likely to experience more tensile force than frictional force, whereas the grafts in Models 1 and 2 experience less tensile force and mainly undergo frictional contact with the tibia. Prolonged large tensile loads may lead to elongation of the graft thus affecting knee stability. Autografts commonly used for PCL reconstruction, such as the hamstring tendon [29], have been reported to have higher ultimate tensile load and stiffness compared to bone-patellar tendon-bone (BTB) autografts and autografts used for ACL reconstruction [30, 31], suggesting that the hamstring tendon has good tensile strength. Zhao et al. reported that the ultimate tensile strength of the PCL is 1800 N, while the ultimate tensile strength of a four-strand hamstring graft is 4000 N [32]. Therefore, we believe that although the soft tissue reference method results in greater tensile force on the graft, it significantly reduces friction, which may help reduce graft wear and lower the risk of surgical failure. However, the threshold of friction that the graft can withstand has not been clearly reported in the literature, so further research is needed regarding the trade-off between tension and friction forces on the graft after clinical surgery. Furthermore, increasing the graft diameter can address the issue of higher tensile forces on the graft. Previous clinical studies have confirmed that the graft diameter for PCLR typically ranges from 8 mm to 12 mm, providing sufficient strength to prevent re-rupture [33]. Rhatomy et al. [34] proposed using fibular long tendon grafts with an average diameter of 8.2 ± 0.6 mm or hamstring tendon grafts with an average diameter of 8.3 ± 0.5 mm, with excellent knee function scores two years postoperatively.

The contact force and effective contact area data in this study demonstrate the advantages of the soft tissue reference positioning method in reducing friction and distributing the load. We calculated the contact force per unit of effective contact area, and the results showed that Model 3 had lower contact force compared to Models 1

and 2. This difference indicates that the soft tissue reference positioning method can more effectively distribute the force on the graft, reducing the occurrence of high-load areas and thus lowering the risk of graft damage. This is consistent with other findings in this study and further supports that the soft tissue reference positioning method can effectively reduce friction between the graft and tibia, lowering the “killer turn” effect. In addition to these advantages, the soft tissue reference tibial tunnel positioning point is located within the anatomical region, which, compared to the Fanelli point, aligns better with physiological structures. Moreover, we established a dual posterior medial (HPM and LPM) approach during surgery using the distal fold of the posterior joint capsule and the posterior septum as references. This approach provides a clear field of vision, reduces the risk of neurovascular injury, and ensures high safety and accuracy. Our preliminary studies have also confirmed this.

There are certain limitations in this study. First, we only used a 3D model from a single volunteer for the analysis, and the single data were not statistically analyzed, which may affect the applicability of the data; future studies should expand the sample size to include individuals of different genders, ages, and body types. Second, this study only simulated a static posterior drawer test, and future research should incorporate dynamic experiments to explore the performance of different positioning methods under various movement conditions. Furthermore, this study is a finite element analysis, and the knee joint model does not completely replicate the tissue properties of the real knee joint, so the actual results should be combined with clinical studies. Previous anatomical and clinical studies have already confirmed the effectiveness and feasibility of the soft tissue-based tibial tunnel positioning method, so the results of this study offer a reasonable degree of credibility and can serve as a valuable reference.

Conclusion

In this study, three-dimensional finite element analysis revealed that compared to PCL reconstruction using the anatomical region center point and Fanelli point, the soft tissue reference tibial positioning method results in greater tensile force on the graft, but significantly reduces the friction between the graft and tibia, which suggest that it may optimize the biomechanical stability of the grafts by decreasing the risk of wear and tear. This study theoretically provides new options for PCL surgical techniques, but these conclusions need to be further validated by long-term clinical follow-up studies.

Acknowledgements

Not applicable.

Author contributions

S T: acquisition of data, analysis of data, draft manuscript; Y Z: analysis of data, review and edit manuscripts; Y L: rework the content, acquisition of data; Y N: analysis of data, rework the content; Z L: acquisition of data, analysis of data; J D: design of research programs, review and edit manuscripts, access to funds.

Funding

This study was supported by the “14th Five-Year” clinical medicine Innovation Research Team Support program of Hebei Medical University(2022LCTD-B25).

Data availability

The raw data of this study support the findings and are available upon reasonable request to the corresponding author. Data requests can be sent to the corresponding author at djt@hebmu.edu.cn.

Declarations

Ethics approval and consent to participate

This study was approved by the ethical review committee of Hebei Medical University Third Hospital, and informed consent was obtained from the participants and their legal guardians. This study adheres to the Declaration of Helsinki.

Consent for publication

Written informed consent for publication of their clinical details and clinical images was obtained from the patient.

Competing interests

The authors declare no competing interests.

Author details

¹Department of Joint Surgery, Hebei Medical University Third Hospital, Shijiazhuang, China

²Institute of Orthopedics, Hebei Medical University Third Hospital, Shijiazhuang, China

Received: 14 February 2025 / Accepted: 30 April 2025

Published online: 06 May 2025

References

- Logan CA, Beaulieu-Jones BR, Sanchez G, et al. Posterior cruciate ligament injuries of the knee at the National football league combine: an imaging and epidemiology study. *Arthroscopy*. 2018;34(3):681–6. <https://doi.org/10.1016/j.arthro.2017.08.304>.
- Donno L, Galluzzo A, Pascale V, et al. Walking with a posterior cruciate ligament injury: A musculoskeletal model study. *Bioeng (Basel)*. 2023;10(10):1178. <https://doi.org/10.3390/bioengineering10101178>. Published 2023 Oct 11.
- Kang KT, Koh YG, Jung M, et al. The effects of posterior cruciate ligament deficiency on posterolateral corner structures under gait- and squat-loading conditions: A computational knee model. *Bone Joint Res*. 2017;6(1):31–42. <https://doi.org/10.1302/2046-3758.61.BJR-2016-0184.R1>.
- Winkler PW, Zsidai B, Wagala NN, et al. Evolving evidence in the treatment of primary and recurrent posterior cruciate ligament injuries, part 2: surgical techniques, outcomes and rehabilitation. *Knee Surg Sports Traumatol Arthrosc*. 2021;29(3):682–93. <https://doi.org/10.1007/s00167-020-06337-2>.
- Moatshe G, LaPrade CM, Fenstad AM, et al. Rates of subjective failure after both isolated and combined posterior cruciate ligament reconstruction: A study from the Norwegian knee ligament registry 2004–2021. *Am J Sports Med*. 2024;52(6):1491–7. <https://doi.org/10.1177/03635465241238461>.
- Fanelli GC, PCL Transtibial Tunnel Reconstruction. *Sports Med Arthrosc Rev*. 2020;28(1):8–13. <https://doi.org/10.1097/JSA.000000000000255>.
- de Queiroz AA, Janovsky C, da Silveira Franciozi CE, et al. Posterior cruciate ligament reconstruction by means of tibial tunnel: anatomical study on cadavers for tunnel positioning. *Rev Bras Ortop*. 2014;49(4):370–3. <https://doi.org/10.1016/j.rboe.2014.04.016>. Published 2014 May 5.
- Okoroafor UC, Saint-Preux F, Gill SW, Bledsoe G, Kaar SG. Nonanatomic tibial tunnel placement for Single-Bundle posterior cruciate ligament reconstruction leads to greater posterior tibial translation in a Biomechanical model. *Arthroscopy*. 2016;32(7):1354–8. <https://doi.org/10.1016/j.arthro.2016.01.019>.
- Teng Y, Jia G, Lu F, et al. Biomechanical comparison of proximal, distal, and anatomic tibial tunnel for transtibial posterior cruciate ligament reconstruction. *Proc Inst Mech Eng H*. 2023;237(1):104–12. <https://doi.org/10.1177/09544119221135935>.
- Bergfeld JA, McAllister DR, Parker RD, et al. A Biomechanical comparison of posterior cruciate ligament reconstruction techniques. *Am J Sports Med*. 2001;29(2):129–36. <https://doi.org/10.1177/03635465010290020401>.
- Nayyar AK, Gupta R. Morphometry of posterior cruciate ligament in knee joint - A cadaveric study. *Clin Ter*. 2023;174(6):525–30. <https://doi.org/10.7417/CT.2023.5020>.
- Jarvis DL, Waterman BR. Editorial commentary: stump sparing or footprint exposing?? Management of the tibial remnant during posterior cruciate ligament reconstruction. *Arthroscopy*. 2019;35(9):2669–70. <https://doi.org/10.1016/j.arthro.2019.05.035>.
- Ahn JH, Lee SH, Choi SH, Wang JH, Jang SW. Evaluation of clinical and magnetic resonance imaging results after treatment with casting and bracing for the acutely injured posterior cruciate ligament. *Arthroscopy*. 2011;27(12):1679–87. <https://doi.org/10.1016/j.arthro.2011.06.030>.
- Lin Y, Huang Z, Zhang K, et al. Lower tibial tunnel placement in isolated posterior cruciate ligament reconstruction: clinical outcomes and quantitative radiological analysis of the killer turn. *Orthop J Sports Med*. 2020;8(8):2325967120923950. <https://doi.org/10.1177/2325967120923950>. Published 2020 Aug 18.
- Wang Z, Xiong Y, Chen G, et al. Modified tibial tunnel placement for single-bundle posterior cruciate ligament reconstruction reduces the killer turn in a Biomechanical model. *Med (Baltim)*. 2019;98(52):e18439. <https://doi.org/10.1097/MD.00000000000018439>.
- Sekiya JK, West RV, Ong BC, Irrgang JJ, Fu FH, Harner CD. Clinical outcomes after isolated arthroscopic single-bundle posterior cruciate ligament reconstruction. *Arthroscopy*. 2005;21(9):1042–50. <https://doi.org/10.1016/j.arthro.2005.05.023>.
- Fanelli GC, Beck JD, Edson CJ. Double bundle posterior cruciate ligament reconstruction: surgical technique and results. *Sports Med Arthrosc Rev*. 2010;18(4):242–8. <https://doi.org/10.1097/JSA.0b013e3181f2faa1>.
- Wang Z, Xiong Y, Li Q, et al. Evaluation of tibial tunnel placement in single case posterior cruciate ligament reconstruction: reducing the graft peak stress may increase posterior tibial translation. *BMC Musculoskelet Disord*. 2019;20(1):521. <https://doi.org/10.1186/s12891-019-2862-z>. Published 2019 Nov 7.
- Niu Y, Li Z, Chen Z, et al. The tibial capsular reflection and septum in posterior compartment are safe and reliable soft-tissue landmark for tibial tunnel drilling in posterior cruciate ligament reconstruction. *Knee Surg Sports Traumatol Arthrosc*. 2024;32(7):1682–9.
- Niu Y, Chen Z, Jin L, et al. A modified anatomical posterior cruciate ligament reconstruction technique using the posterior septum and posterior capsule as landmarks to position the low tibial tunnel. *BMC Musculoskelet Disord*. 2024;25(1):73.
- Jia G, Tang Y, Liu Z, et al. 3D killer turn angle in transtibial posterior cruciate ligament reconstruction is determined by the graft turning angle both in the sagittal and coronal Planes. *Orthop Surg*. 2022;14(9):2298–306. <https://doi.org/10.1111/os.13411>.
- Teng Y, Da L, Jia G, et al. What is the maximum tibial tunnel angle for transtibial PCL reconstruction?? A comparison based on virtual radiographs, CT images, and 3D knee models. *Clin Orthop Relat Res*. 2022;480(5):918–28. <https://doi.org/10.1097/CORR.0000000000002111>.
- Yang F, Yokoe T, Ouchi K, Tajima T, Chosa E. Influence of the tibial tunnel angle and posterior tibial slope on killer turn during posterior cruciate ligament reconstruction: A Three-Dimensional finite element analysis. *J Clin Med*. 2023;12(3):805. <https://doi.org/10.3390/jcm12030805>.
- Kim SJ, Shin JW, Lee CH, et al. Biomechanical comparisons of three different tibial tunnel directions in posterior cruciate ligament reconstruction. *Arthroscopy*. 2005;21(3):286–93. <https://doi.org/10.1016/j.arthro.2004.11.004>.
- Li Y, Zhang J, Song G, Li X, Feng H. The mechanism of killer turn causing residual laxity after transtibial posterior cruciate ligament reconstruction. *Asia Pac J Sports Med Arthrosc Rehabil Technol*. 2016;3:13–8. <https://doi.org/10.1016/j.asmart.2015.12.001>.
- LaPrade CM, Civitaresse DM, Rasmussen MT, LaPrade RF. Emerging updates on the posterior cruciate ligament: A review of the current literature. *Am J Sports Med*. 2015;43(12):3077–92. <https://doi.org/10.1177/0363546515572770>.
- Huang TW, Wang CJ, Weng LH, Chan YS. Reducing the killer turn in posterior cruciate ligament reconstruction. *Arthroscopy*. 2003;19(7):712–6. [https://doi.org/10.1016/s0749-8063\(03\)00394-3](https://doi.org/10.1016/s0749-8063(03)00394-3).

28. Zhang X, Teng Y, Yang X, et al. Evaluation of the theoretical optimal angle of the tibial tunnel in transtibial anatomic posterior cruciate ligament reconstruction by computed tomography. *BMC Musculoskeletal Disord.* 2018;19(1):436. <https://doi.org/10.1186/s12891-018-2348-4>.
29. Yılmaz B, Özdemir G, Keskinöz EN, Tümentemur G, Gökkuş K, Demiralp B. Comparing dimensions of Four-Strand hamstring tendon grafts with native anterior and posterior cruciate ligaments. *Biomed Res Int.* 2016;2016:3795367. <https://doi.org/10.1155/2016/3795367>.
30. Lin KM, Boyle C, Marom N, Marx RG. Graft selection in anterior cruciate ligament reconstruction. *Sports Med Arthrosc Rev.* 2020;28(2):41–8. <https://doi.org/10.1097/JSA.0000000000000265>.
31. Mehran N, Moutzouros VB, Bedi A. A review of current graft options for anterior cruciate ligament reconstruction. *JBJS Rev.* 2015;3(11):e2. <https://doi.org/10.2106/JBJS.RVW.O.00009>.
32. Zhao J, Huangfu X. Arthroscopic single-bundle posterior cruciate ligament reconstruction: retrospective review of 4- versus 7-strand hamstring tendon graft. *Knee.* 2007;14(4):301–5. <https://doi.org/10.1016/j.knee.2007.03.008>.
33. Koh JRD, Loh SYJ. All-inside posterior cruciate ligament reconstruction - A systematic review of current practice. *J Orthop.* 2024;55:1–10. <https://doi.org/10.1016/j.jor.2024.03.041>.
34. Rhatomy S, Abadi MBT, Setyawan R, et al. Posterior cruciate ligament reconstruction with peroneus longus tendon versus hamstring tendon: a comparison of functional outcome and donor site morbidity. *Knee Surg Sports Traumatol Arthrosc.* 2021;29(4):1045–51. <https://doi.org/10.1007/s00167-020-06077-3>.

Publisher's note

Springer Nature remains neutral with regard to jurisdictional claims in published maps and institutional affiliations.